

GC14-07: Nonlinear Interactions between Climate and Atmospheric Carbon Dioxide Drivers of Terrestrial and Marine Carbon Cycle Changes

Forrest M. Hoffman^{1,2}, James T. Randerson², J. Keith Moore², Michael L. Goulden²,
Weiwei Fu², Charles D. Koven³, Abigail L. S. Swann⁴, Natalie M. Mahowald⁵,
Keith Lindsay⁶, and Ernesto Muñoz⁶

¹Oak Ridge National Laboratory, ²University of California Irvine, ³Lawrence Berkeley National Laboratory,
⁴University of Washington Seattle, ⁵Cornell University, and ⁶National Center for Atmospheric Research

December 11, 2017, 17:30–17:45

 **AGU FALL MEETING**

New Orleans
11-15 Dec. 2017 What will *you* discover?



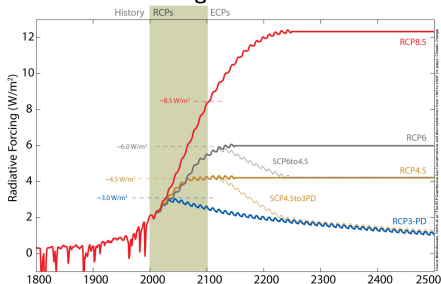
CLIMATE CHANGE
SCIENCE INSTITUTE
OAK RIDGE NATIONAL LABORATORY



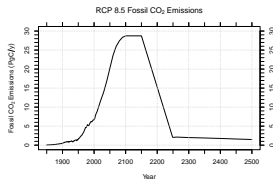
Science Question

To what degree do the effects of climate change due to warming and CO₂ fertilization in isolation combine linearly?

Radiative Forcing for RCPs and ECPs



Meinshausen et al. (2011) extended RCP forcings out to 2500.



$$\Delta C_0 = \beta_0 \Delta \text{CO}_2 + \gamma_0 \Delta T$$

$$\Delta C_L = \beta_L \Delta \text{CO}_2 + \gamma_L \Delta T$$

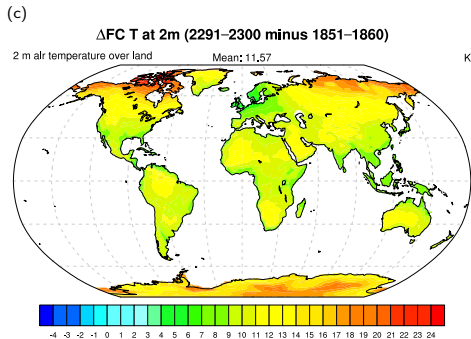
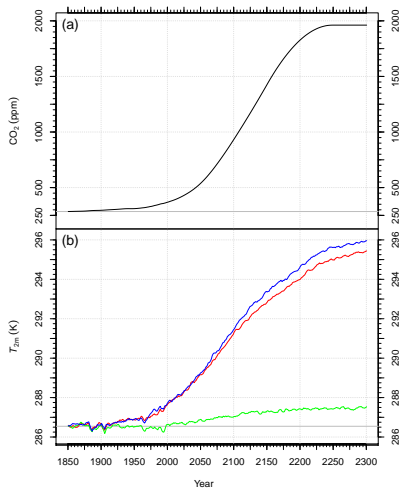
$$g = \frac{-\alpha(\gamma_0 + \gamma_L)}{(m + \beta_0 + \beta_L)}$$

From Friedlingstein et al. (2006).

Simulation Identifier	Radiative Coupling		Biogeochemical Coupling			Experiment Name
	CO ₂	Other GHG & aerosols	CO ₂	Nitrogen deposition	Land use	
RAD	✓	✓	—	—	—	bcrd
BGC	—	—	✓	✓	—	bdracs.pftcon
FC	✓	✓	✓	✓	—	bdrd.pftcon

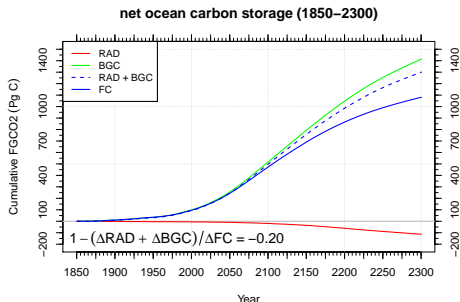
- ✓ Transient anthropogenic forcing
- Constant pre-industrial (1850) forcing

Climate–Carbon Cycle Drivers (1850–2300)

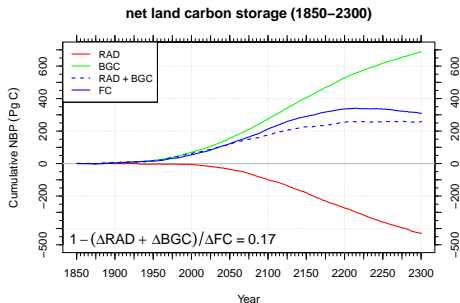


- (a) Prescribed atmospheric CO₂ mole fraction was stabilized at 1962 ppm around 2250.
(b) 2 m air temperature increased by 9.4°C in **FC**, 8.9°C in **RAD**, and 1.0°C in **BGC** simulations.
(c) Mean air temperature over land increased by 11.6°C in the **FC** simulation and approached 25°C at high latitudes.

Net Ocean and Land Carbon Uptake (1850–2300)



Net ocean carbon storage has a nonlinear response that Schwinger et al. (2014) attributed to surface stratification under climate change that restricted C penetration into intermediate and deep waters.



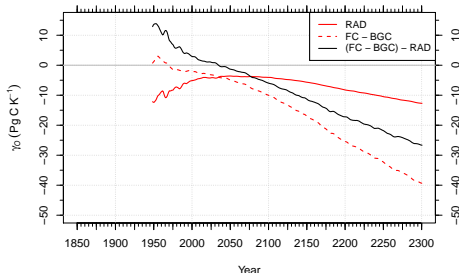
Net land carbon storage also has a nonlinear response, of opposite sign, that has not been explored in ESMs, although Zickfeld et al. (2011) explored similar nonlinear responses in an EMIC. It is driven by larger than expected productivity increases due to positive hydrological and nitrogen mineralization feedbacks.

Ocean and Land Climate–Carbon Sensitivities

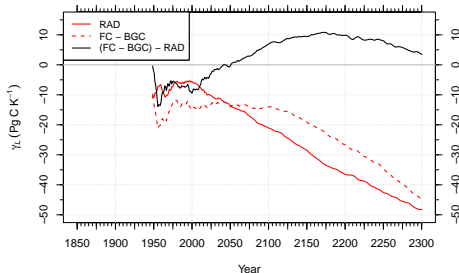
The difference between the net ocean carbon storage climate sensitivities, γ_O^{RAD} and $\gamma_O^{\text{FC-BGC}}$, was nearly -27 Pg C K^{-1} and continued to diverge at the end of the 23rd century.

The difference between the net land carbon storage climate sensitivities, γ_L^{RAD} and $\gamma_L^{\text{FC-BGC}}$, peaked at about 10 Pg C K^{-1} around 2175 and ended at about 4 Pg C K^{-1} at 2300.

net ocean carbon storage climate sensitivity (1850–2300)

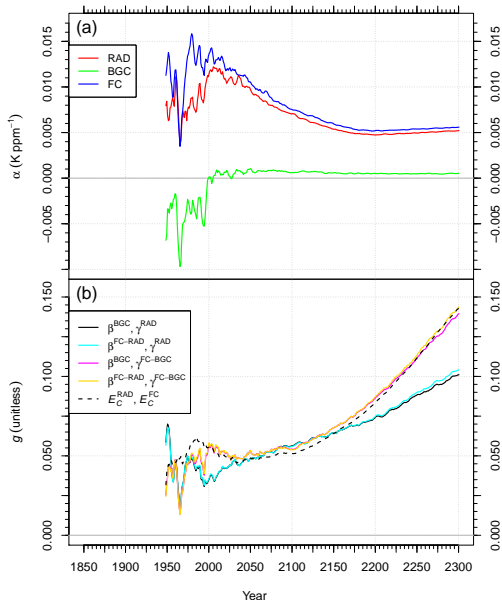


net land carbon storage climate sensitivity (1850–2300)



Climate Sensitivities and Climate–Carbon Cycle Gains

Climate Sensitivities and Feedback Gains (1850–2300)

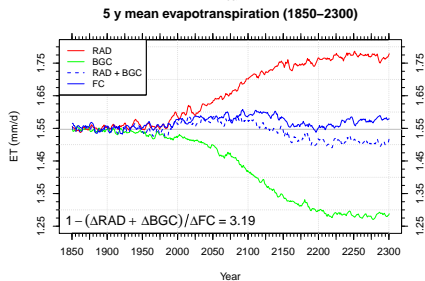
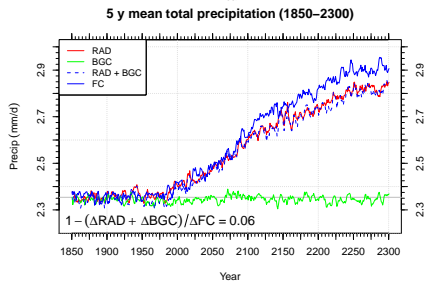
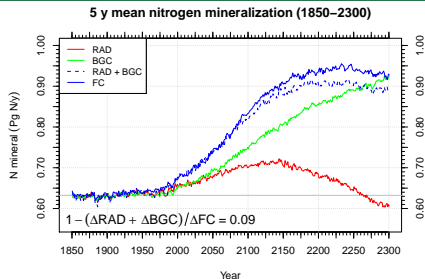
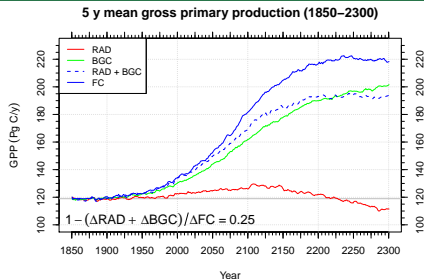


The climate sensitivity, α , for the **FC** simulation was about 0.0056 K ppm⁻¹ at the end of the 23rd century.

The climate–carbon cycle gain* (g) clustered around two different values, depending on the method and experiments used to calculate it, and at 2300 was 42% higher when estimated from sensitivity parameters derived from (**FC** – **BGC**) than from **RAD**.

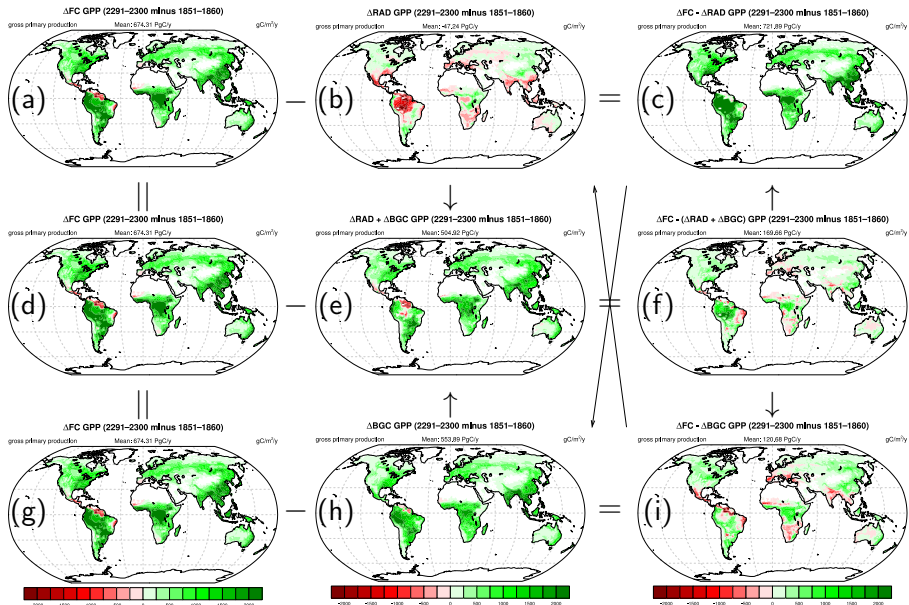
*This gain included effects of aerosols and other greenhouse gases.

Drivers of Nonlinear Terrestrial Uptake Responses

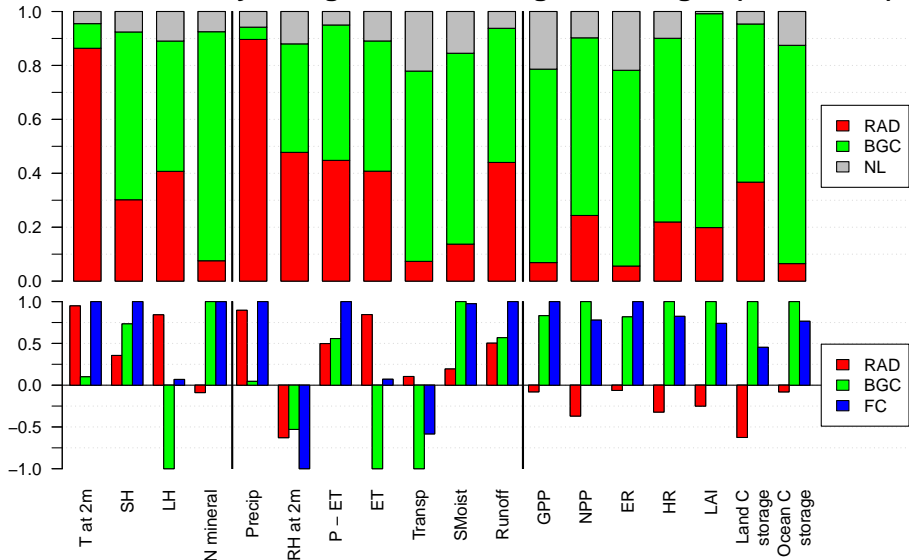


Enhanced gross primary production (GPP) and higher rates of N mineralization, driven by excess precipitation increases and reduced evapotranspiration, led to the nonlinear C uptake response on land under simultaneous climate change and elevated CO₂ levels.

Nonlinear GPP Responses Across Model Experiments



Drivers of Hydrological and Ecological Changes (1850–2300)



Energy & N

Water

Carbon

Summary and Conclusions

Science Question

To what degree do the effects of climate change due to warming and CO₂ fertilization in isolation combine linearly?

- ▶ **RAD** simulations yielded a net ocean carbon storage climate sensitivity (γ_O) that was weaker and a net land carbon storage sensitivity (γ_L) that was stronger than those diagnosed from **FC** and **BGC** simulations.
 - ▶ For the ocean, the nonlinearity was associated with warming-induced weakening of ocean circulation and mixing, which limited exchange of dissolved inorganic carbon between surface and deeper water masses.
 - ▶ For the land, the nonlinearity was associated with strong gains in gross primary production in the **FC** simulation, driven by enhancements in the hydrological cycle and increased nutrient availability.
- ▶ The feedback gain* (g) at 2300 was 42% higher when estimated from sensitivity parameters derived from (**FC** – **BGC**) than from **RAD**.
- ▶ We recommend deriving $\gamma_O^{\text{FC-BGC}}$ and $\gamma_L^{\text{FC-BGC}}$ in future studies.

*This gain included effects of aerosols and other greenhouse gases.

Acknowledgments



U.S. DEPARTMENT OF
ENERGY

Office of Science



This research was supported by the Biogeochemistry–Climate Feedbacks (BGC Feedbacks) Scientific Focus Area, which is sponsored by the Regional and Global Climate Modeling Program in the Climate and Environmental Sciences Division (CESD) of the Biological and Environmental Research (BER) Program in the U.S. Department of Energy Office of Science, and by the National Science Foundation (AGS-1048890). This research used resources of the National Center for Computational Sciences (NCCS) at Oak Ridge National Laboratory (ORNL), which is managed by UT-Battelle, LLC, for the U.S. Department of Energy under Contract No. DE-AC05-00OR22725.

References

- P. Friedlingstein, P. M. Cox, R. A. Betts, L. Bopp, W. von Bloh, V. Brovkin, S. C. Doney, M. Eby, I. Fung, B. Govindasamy, J. John, C. D. Jones, F. Joos, T. Kato, M. Kawamiya, W. Knorr, K. Lindsay, H. D. Matthews, T. Raddatz, P. Rayner, C. Reick, E. Roeckner, K.-G. Schnitzler, R. Schnur, K. Strassmann, S. Thompson, A. J. Weaver, C. Yoshikawa, and N. Zeng. Climate-carbon cycle feedback analysis, results from the C⁴MIP model intercomparison. *J. Clim.*, 19(14):3373–3353, July 2006. doi:10.1175/JCLI3800.1.
- M. Meinshausen, S. Smith, K. Calvin, J. Daniel, M. Kainuma, J.-F. Lamarque, K. Matsumoto, S. Montzka, S. Raper, K. Riahi, A. Thomson, G. Velders, and D. P. van Vuuren. The RCP greenhouse gas concentrations and their extensions from 1765 to 2300. *Clim. Change*, 109(1): 213–241, Nov. 2011. doi:10.1007/s10584-011-0156-z.
- J. Schwinger, J. F. Tjiputra, C. Heinze, L. Bopp, J. R. Christian, M. Gehlen, T. Ilyina, C. D. Jones, D. Salas-Méllia, J. Segschneider, R. Séférian, and I. Totterdell. Nonlinearity of ocean carbon cycle feedbacks in CMIP5 Earth system models. *J. Clim.*, 27(11):3869–3888, June 2014. doi:10.1175/JCLI-D-13-00452.1.
- K. Zickfeld, M. Eby, H. D. Matthews, A. Schmittner, and A. J. Weaver. Nonlinearity of carbon cycle feedbacks. *J. Clim.*, 24(16):4255–4275, Aug. 2011. doi:10.1175/2011JCLI3898.1.

Century-by-Century Carbon & Temperature Changes

Variable	Time (year)			
	2000	2100	2200	2300
$[\text{CO}_2]_A$ (ppm)	369	936	1829	1962
Variable	Time Period (years)			
	1850–2000	1850–2100	1850–2200	1850–2300
$\Delta T_{2m}^{\text{RAD}}$ (K)	1.13	4.76	7.46	8.90
$\Delta T_{2m}^{\text{BGC}}$ (K)	0.10	0.50	0.87	0.99
$\Delta T_{2m}^{\text{FC}}$ (K)	1.19	4.92	8.11	9.41
ΔC_O^{RAD} (Pg C)	–6	–19	–62	–113
ΔC_O^{BGC} (Pg C)	100	519	1050	1414
ΔC_O^{FC} (Pg C)	97	475	866	1082
ΔC_L^{RAD} (Pg C)	–8	–100	–275	–430
ΔC_L^{BGC} (Pg C)	69	276	529	687
ΔC_L^{FC} (Pg C)	55	213	336	309
E_C^{RAD} (Pg C)	167	1265	2948	3023
E_C^{BGC} (Pg C)	349	2180	4862	5663
E_C^{FC} (Pg C)	331	2072	4486	4955

Climate–Carbon Cycle Feedback Parameters and Gains

Parameter	Time Period (years)			
	1850–2000	1850–2100	1850–2200	1850–2300
α (K ppm ⁻¹)	0.0140	0.0075	0.0052	0.0056
β_O^{BGC} (Pg C ppm ⁻¹)	1.19	0.80	0.68	0.84
$\beta_O^{\text{FC-RAD}}$ (Pg C ppm ⁻¹)	1.23	0.76	0.60	0.71
β_L^{BGC} (Pg C ppm ⁻¹)	0.84	0.42	0.34	0.41
$\beta_L^{\text{FC-RAD}}$ (Pg C ppm ⁻¹)	0.72	0.48	0.39	0.44
γ_O^{RAD} (Pg C K ⁻¹)	-5.10	-4.06	-8.26	-12.69
$\gamma_O^{\text{FC-BGC}}$ (Pg C K ⁻¹)	-2.22	-10.06	-25.47	-39.37
γ_L^{RAD} (Pg C K ⁻¹)	-5.70	-21.09	-36.54	-48.25
$\gamma_L^{\text{FC-BGC}}$ (Pg C K ⁻¹)	-15.00	-14.05	-26.69	-44.77
$g(\beta^{\text{BGC}}, \gamma^{\text{RAD}})$	0.035	0.056	0.075	0.101
$g(\beta^{\text{FC-RAD}}, \gamma^{\text{RAD}})$	0.036	0.056	0.075	0.104
$g(\beta^{\text{BGC}}, \gamma^{\text{FC-BGC}})$	0.057	0.054	0.087	0.139
$g(\beta^{\text{FC-RAD}}, \gamma^{\text{FC-BGC}})$	0.058	0.053	0.087	0.144
$g(E_C^{\text{RAD}}, E_C^{\text{FC}})$	0.056	0.051	0.084	0.143